

Numerical and Experimental Study on the Effect of Weak layer Parameters and Overburden on the Bearing Capacity of Circular Footing

Mehrshad Hosseini Fani ¹, Ahad Bagherzadeh Khalkhali ^{2*}, Navid Ganjian ³

1- Ph.D. candidate, Department of Civil Engineering, Science And Research Branch, Islamic Azad University, Tehran, Iran

2- Assistant Professor, Department of Civil Engineering, Science And Research Branch, Islamic Azad University, Tehran, Iran

3- Assistant Professor, Department of Civil Engineering, Science And Research Branch, Islamic Azad University, Tehran, Iran

ABSTRACT

The bearing capacity of circular footings on layered soil masses with weak soil layers is a crucial issue in geotechnical engineering. In this paper, a numerical and experimental investigation was conducted to study the effect of weak layer parameters and overburden on the bearing capacity of circular footings. A small-scale physical model was used to conduct experimental tests, while numerical simulations were performed using a finite element method software package. The experimental and numerical results were compared, and the findings were in strong agreement with one another. The study showed that the presence of a weak layer in the soil significantly reduces the bearing capacity of circular footings. The thickness, depth, and overburden of the weak layer were found to have a significant impact on the bearing capacity of the footing. In this study, the buried depth of weak layer was 8 cm, where the depth-to-diameter ratio of the footing is equal to one. At this depth, the weak lens layer also affects the bearing capacity, and depending on its thickness, it results in a decrease in bearing capacity by 14 to 19 percent. The effect of one-sided loading in the presence of a weak layer in the bed is greater than in a homogeneous bed. The presence of asymmetric overburden substantially reduces the negative impact of the weak lens. The paper provides insights into the behavior of circular footings on layered soil masses with weak soil layers, which can help in designing more reliable and cost-effective foundations.

ARTICLE INFO

Receive Date: 15 June 2024

Revise Date: 23 August 2024

Accept Date: 26 September 2024

Keywords:

bearing capacity
weak layer
circular footing
layered soil mass
finite element analysis
model tests

All rights reserved to Iranian Society of Structural Engineering.

doi: [10.22065/jsce.2024.462887.3443](https://doi.org/10.22065/jsce.2024.462887.3443)

*Corresponding author: Ahad bagherzadeh khalkhali.

Email address: a-bagherzadeh@srbiau.ac.ir

Notations

B	footing width
c'	cohesion
C_c	coefficient of curvature
C_u	uniformity coefficient
D_{max}	maximum grain size
D_f	embedment depth of foundation
D_r	relative density
D_{10}	effective grain size
D_{50}	average grain size
G_s	specific gravity
N_γ, N_q	bearing capacity factors
q'	overburden
q_{ult}	Ultimate bearing capacity of uniform sand
q_u	Ultimate bearing capacity of foundation
q_{uw}	The ultimate bearing capacity of footings resting on subsoils consisting of a weak sand layer
Z_i	depth from the ground surface of thin layer
T	thickness of thin layer
γ	unit weight
γ_d	dry unit weight
γ_{dmax}	maximum dry unit weight
γ_{dmin}	minimum dry unit weight
φ'	angle of internal friction
τ	shear stress
σ_n	normal stress
σ_v	vertical stress

1. Introduction

The foundation of a structure is a critical component that bears its weight and is subject to varying stresses from different sources and angles. The bearing capacity of a foundation depends on a variety of factors such as soil properties, geometry of the foundation, and the loads applied to it. A weak layer located within the soil mass can have a significant impact on the bearing capacity of the foundation, especially for circular footings. The presence of a weak layer can cause differential settlement, which can result in the failure of the foundation and ultimately the structure. Therefore, it is essential to investigate the effect of weak layer parameters and overburden on the bearing capacity of circular footings on layered soil masses with weak soil layers. The effect of weak soil layers on the bearing capacity of footings has been a subject of extensive research in geotechnical engineering. Several studies have been conducted to investigate the behavior of circular footings on layered soil masses with weak soil layers.

As mentioned above, only a few researchers have studied the impact of the weak layer on the bearing capacity of shallow foundations. Most studies have not investigated the effect of overburden loads on the foundation's bearing capacity. In cases where the effect of overburden load has been studied, it has been symmetrical. This study aims to investigate the effect of asymmetric loads on different thicknesses and depths of the weak layer. Numerical modeling has also been utilized to examine the impact of weak layers and asymmetric overhead load on the failure mechanism. The outcomes obtained from physical and numerical models are contrasted and compared with those of analytical methods. One of the innovations in this article is the comparison of physical and numerical models with analytical methods while considering asymmetric overburden.

2. literature Review

Numerical and experimental studies have been conducted to investigate the effect of weak soil layers on the bearing capacity of footings. For instance, Ahmad and Khalafalla [1] conducted a numerical study to investigate the effect

of weak soil layers on the bearing capacity of shallow foundations. The study revealed that the presence of weak soil layers reduces the bearing capacity of the foundation. In addition to the above studies, several researchers have also investigated the effect of overburden on the bearing capacity of footings resting on weak layers. For example, Amin and Adhikary [2] investigated the effect of overburden pressure on the bearing capacity of shallow footings. The study showed that the bearing capacity of the footing decreases with an increase in overburden pressure. Furthermore, experimental studies have also been conducted to investigate the effect of weak soil layers on the bearing capacity of footings. For instance, Arora et al. [3] conducted a laboratory experiment to investigate the bearing capacity of circular footings on layered soil with a weak layer. The results signified the presence of a weak soil layer significantly reduces the bearing capacity of the footing. Similarly, Behera et al. [4] conducted a laboratory experiment to investigate the bearing capacity of shallow foundations on weak soil layers. The study showed that the bearing capacity of the footing decreases with an increase in the thickness of the weak soil layer.

Other researchers have investigated the effect of reinforcement on the bearing capacity of footings resting on weak soil layers. For example, Abd Elaziz et al. [5] investigated the effect of geogrid reinforcement on the bearing capacity of circular footings on soft clay with a sandy soil layer. The results showed that geogrid reinforcement improves the bearing capacity of the footing and reduces the settlement. Moreover, the effect of weak soil layer parameters on the bearing capacity of footings has also been investigated. For example, Al-Sammarrarie and Al-Rawas [6] conducted a study to investigate the effect of the shear strength parameters of the weak soil layer on the bearing capacity of footings. The study showed that the bearing capacity of the footing decreases with a decrease in the shear strength of the weak soil layer.

In addition to the above studies, the effect of the shape of the footing on the bearing capacity of footings on layered soil with weak soil layers has also been investigated. For instance, Huang et al. [7] conducted a numerical study to investigate the effect of the footing shape on the bearing capacity of footings on layered soil with a weak layer. The results showed that the footing shape significantly affects the bearing capacity of the footing on layered soil with weak soil layers.

Lastly, several researchers have also investigated the behavior of group footings on layered soil masses with weak soil layers. For example, Khamchhiyan et al. [8] conducted a numerical study to investigate the behavior of group footings on layered soil with a weak layer. The study revealed that the bearing capacity of group footings is significantly influenced by the presence of a weak soil layer. Ullah et al. [9] presents a numerical study on the behavior of a rectangular footing placed on a sand embankment over mine tailings. The study used a finite element method to investigate the effect of the thickness of the sand layer and the height of the tailings on the bearing capacity and settlement of the footing. The study found that the bearing capacity increased with increasing sand thickness, while the settlement decreased. Additionally, the study found that the bearing capacity decreased with increasing tailings height, while the settlement increased. The results of this study can be useful in designing foundations on mine tailings and similar materials. The issue of bearing capacity of shallow foundation on multi-layered subgrade is raised as an important discussion in geotechnical research, for example, it can be mentioned the research required in 2023 [10-11] used Abaqus software to investigate the bearing capacity of the shallow foundation on the two-layer subgrade under the effect of combined loadings. Yadav et al. [12], Bhardwaj et al. [13] and Buragadda et al. [14] conducted numerical and physical studies on the bearing capacity of the shallow foundation based on layered sand soil and They investigated the effects of layer thickness, layer reinforcement and foundation width on the behavior of shallow foundation. Eshkevari et al. [15] investigates the bearing capacity of strip footings on layered sands using numerical modeling. The study aims to evaluate the influence of the number and thickness of sand layers on the bearing capacity of the footing. The authors used the finite element method to simulate the behavior of strip footings on layered sand deposits and examined the impact of different parameters, including the footing width, depth, and eccentricity. The results showed that the presence of a weak sand layer could significantly reduce the bearing capacity of the footing. The study also highlights the importance of considering the number and thickness of sand layers in the design of strip footings on layered sand deposits to ensure their safe and economic performance. Another similar study was conducted by Hanna, Farah, and Abdel-Rahman [16] investigates the behavior of shallow foundations resting on strong sand overlying weak sand. The study used finite element analysis to evaluate the bearing capacity of shallow foundations on layered sand deposits. The results showed that the presence of a strong sand layer overlying a weak sand layer can increase the bearing

capacity of shallow foundations. The study also found that the presence of a weak sand layer underlying a strong sand layer can significantly reduce the bearing capacity of shallow foundations.

Based on the study conducted by Haghsheno et al. [17], the presence of a lens in a state of vibration can have a significant impact on the seismic bearing capacity of shallow strip footings on sand deposits with weak inter-layer. The study examined the effect of the lens and various factors such as weight and resistance parameters of the materials used. The mechanism of failure was considered and the ultimate bearing capacity was determined by taking into account various pressures such as the surcharge pressure, active lateral pressure, and soil resistance pressure. The seismic force was considered as two coefficients, horizontal and vertical, and the effect of the coefficients was included in the calculations. The study suggests that the capacity of static and dynamic bearing capacity of shallow strip footings on sand deposits with weak inter-layer can be easily determined using the equivalent bearing capacity factor.

The article by Peng and Peng [18] presents a slip-line method for determining the ultimate bearing capacity of shallow strip footings. The slip-line method is a classical approach for solving plasticity problems in soils, and it has been widely used to determine the bearing capacity of foundations. The slip-line method is validated through comparisons with experimental results and other analytical solutions. The results show that the proposed method can accurately predict the ultimate bearing capacity of shallow strip footings under various loading conditions.

In conclusion, the presence of a weak soil layer significantly affects the bearing capacity of circular footings on layered soil masses. The parameters that influence the effect of weak soil layers on the bearing capacity of the footing include the thickness of the weak soil layer, overburden pressure, soil types, reinforcement, weak soil layer parameters, footing shape, and group footings. Understanding the behavior of circular footings on layered soil masses with weak soil layers is essential in the design of shallow foundations.

2. Methodology

To investigate the effect of weak layer parameters and overburden on the bearing capacity of circular footings on layered soil masses with weak soil layers, both numerical and experimental studies were conducted. The methodology of each study is described below.

2.1 Experimental Setup

The problem being addressed in this study involves a circular rigid footing that initially rests on the ground surface with no embedment depth, and which is subjected to surcharge loading on a layered soil consisting of dry sand and a thin weak layer. The weak layer has a thickness of T and is composed of a material that is weaker than the surrounding sand and is located at depth Z_i . The schematic diagram of the problem is presented in Figure 1, where plane strain conditions are considered. As shown in the figure, the upper and lower layers of the weak layer consist of sand, and the asymmetrical overburden is represented by the surcharge loading on the physical model. Section view of the physical model is shown in Figure 2.

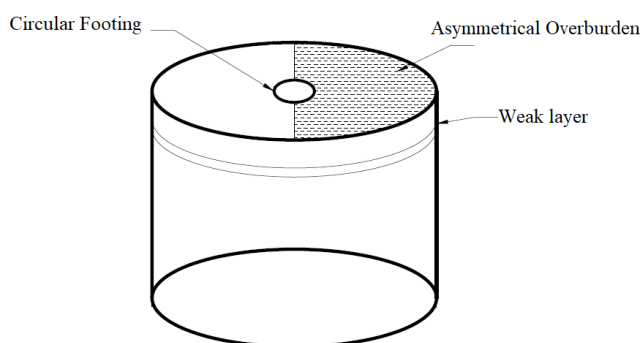


Fig 1. General layout of the circular foundation in experimental modeling.

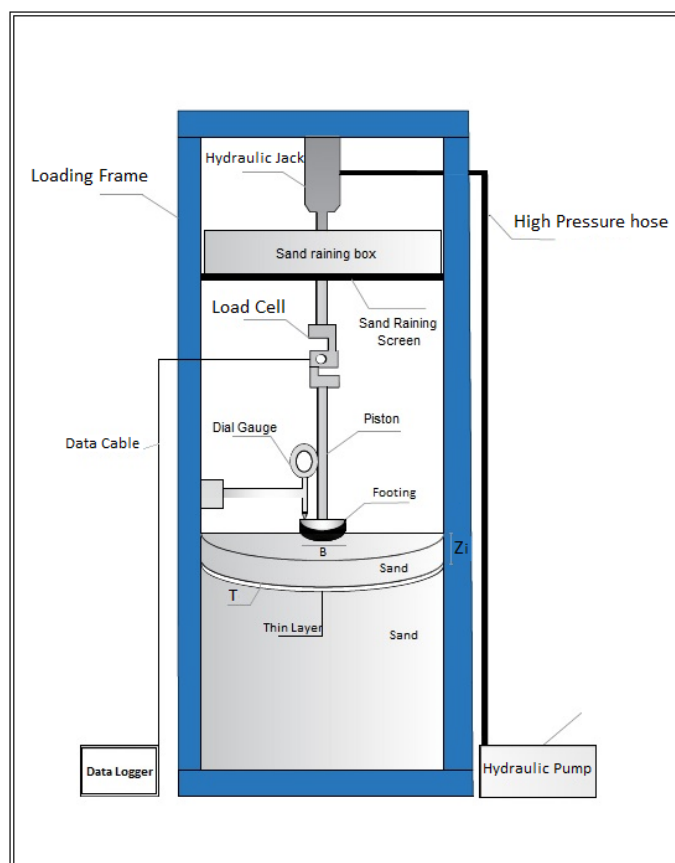


Fig 2. Section view of the physical model

To investigate the bearing capacity of the footing, a study was conducted that varied the thickness and depth of the weak layer ($Z_i = 0, 4, 8\text{cm}$, $T = 0, 7, 14\text{mm}$), as well as the surcharge loading of the foundation, which was set to $q = 0, q, 2q$, and $3q$. The type of material used for the weak layer was also varied. Crushed silica sand (SP) with medium density was used for the bed sand, while materials with different strength properties were used for the weak layer.

To conduct the experiments, a small-scale physical model was designed and built, as shown in Figure 3. The model was built using steel and had a cylindrical shape to simulate a circular foundation. The model had a diameter of 80 mm and was positioned on the surface of the soil mass. The inside available space of the model was 70 cm in diameter and 70 cm in height. The model was filled with layers of sand with a thickness of 7 cm, which were compacted according to the desired relative density. The filling process was repeated until the level below the foundation was reached.

The settlement of the footing was measured using a dial gauge installed on the loading cell, while a hydraulic jack was used to transfer the pressure to the foundation at a constant rate of 1 mm/min. A load cell was used to record the load applied by the hydraulic jack, and the data acquisition system, consisting of a data logger and computer software, was used to extract the load and displacement data for analysis.

To maintain a consistent density of the sand during the filling process, a sand raining screen device was installed directly above the sand mass, and the sand was deposited in 7 cm thick layers using the raining method. The density of the sand was controlled by placing cans of specified volume in different locations of the box.



Fig 3. Circular foundation physical model system detail

It should be noted that the use of a manual hydraulic jack for load application may cause a variation in the loading rate, but under static loading conditions, the effect on the settlement and bearing capacity of the surface footing is insignificant (Bildik and Laman [19]).

The initial step of the test involved installing a sand raining screen device above the sand mass. The sand was then deposited in 7 cm thick layers using the raining method, while the density of the sand was controlled by placing cans of specified volume in different locations of the box. The sand foundation was then formed with defined height and thickness, and the weak layer was made at the same defined depth. Subsequently, sand layers were poured up to the required level, followed by placing the foundation model at a specific location on the surface of the sandy bed. The vertical pressure was then transferred to the foundation model using a manual hydraulic jack at a constant rate of 1 mm/min, and the vertical settlement was measured using a dial gauge with a precision of 0.01 mm. To ensure the reliability of the experiment results, some of the tests were repeated.

The materials used in this study include silica sand for the soil layer and compressible clay powder for the weak layer. The silica sand was obtained from a factory located in Firuzkuh and was air-dried before use. The sand is classified as poorly graded sand (SP) according to the Unified Soil Classification System (USCS) and has a uniform relative density achieved by pouring it from the same fall height using the dry raining method. The physical properties of the sand are shown in Table 1 and the grading curve is presented in Figure 4.

Previous research has indicated that the degree of particle crushing in poorly graded silica sand tends to decrease as the fines content increases. However, due to the low stress level in the tested physical models and the mineralogy and grading of the sand used in this study, particles crushing during the experiments is considered negligible. The shear strength parameters of the sand were determined by seven direct shear tests in accordance with ASTM D 3080 and are a function of the effective stress level. The results of the direct shear test for the sand corresponding to the model stress levels ($1 \text{ kPa} < \sigma_v < 4 \text{ kPa}$) are presented in Figure 5.

The weak layer, which has lower shear strength properties than the sandy bed, was composed of compressible clay powder with CL classification. The clay powder was used continuously in all experiments with a natural moisture content of 6.5%. The physical properties of the clay material are shown in Table 3. The shear strength parameters of the weak layer material were determined by seven direct shear tests, and the results indicate that the shear strength parameters of the weak layer are not affected by the stress level. The direct shear test results for the weak layer material related to the stress levels of the model ($1 \text{ kPa} < \sigma_v < 4 \text{ kPa}$) are presented in Figure 6.

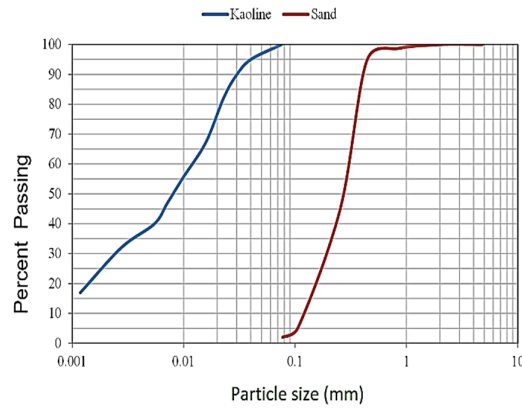


Fig. 4 Particle-size distribution curve for sand

Table 1. Properties of sand used in the model tests

Property	Value	Standard No
Maximum grain size, D_{max} (mm)	2.38	
Diameter corresponding to 60% finer, D_{60}	1.45	
Average grain size, D_{50} (mm)	1.25	
Diameter corresponding to 30%, D_{30} (mm)	0.9	ASTM D C136
Effective grain size, D_{10} (mm)	0.67	
Uniformity coefficient, C_u	2.43	
Coefficient of curvature, C_c	0.88	
Specific gravity, G_s	2.6	ASTM D 854
Maximum dry unit weight, γ_{dmax} (kN/m ³)	19.85	ASTM D 4254
Minimum dry unit weight, γ_{dmin} (kN/m ³)	13.73	ASTM D 4253
Dry unit weight, γ_d (kN/m ³)	16.5	
Relative density, D_r (%)	40	
Classification (USCS)	SP	ASTM D 2487

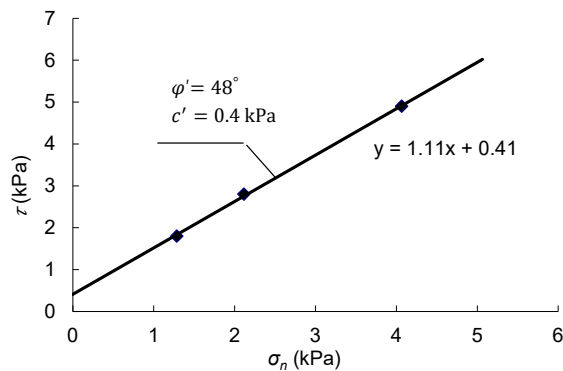
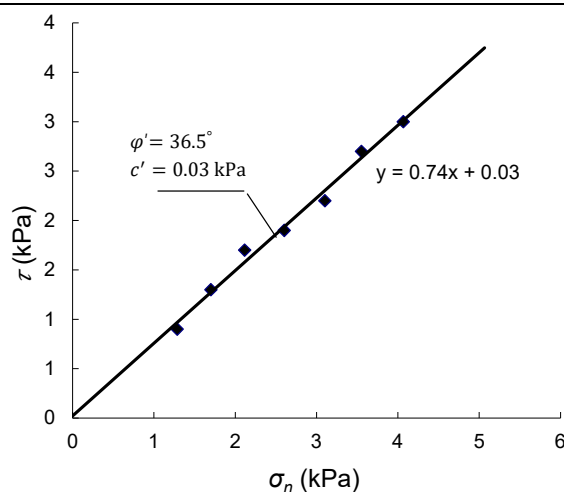


Fig. 5 Results of direct shear test on sand bed at low effective stresses ($1 \text{ kPa} < \sigma_v < 4 \text{ kPa}$)

Table 2. Physical properties of weak layer used in the model tests

Property	Value	Standard No.
Specific gravity, G_s	2.66	ASTM D854
Unit weight, γ (kN/m ³)	12.1	ASTM D6683
Liquid limit (%)	27	
Plastic limit (%)	17	ASTM D4318
Plasticity index (%)	10	
Classification (USCS)	CL	ASTM D2487
Water content (%)	5.5	ASTM D2216

Fig 6. Results of direct shear test on weak layer at low effective stresses ($1 \text{ kPa} < \sigma_v < 4 \text{ kPa}$)

2.2 Numerical method

Numerical simulations were performed using the finite element code ABAQUS 3D to analyze the bearing capacity factors of a reduced-scale physical model. In 2023 Bakhshandeh and Niazmandi [20] show the effects of soil properties on the seismic response of the structure using Finite Element Analysis (FE) (Abaqus). Their research shows the high capacity and acceptable efficiency of Abaqus software for numerical modeling.

Instead of load-displacement curves, a uniform vertical settlement of the footing base was imposed to simulate the real experimental procedure, accounting for the high stiffness of the footing and the roughness of its base. The simple elastic-perfectly plastic Mohr-Coulomb constitutive model with non-associated flow rule was adopted for the soils, which is a widely used model in the literature. This model can accurately predict the shear failure of soil mass. The initial conditions for the model are obtained through geostatic analysis, which requires inputting the soil's lateral pressure coefficient into the software. This coefficient has a value of $1 - \sin \phi$. Once the initial stresses are set up, compressive stress is applied on one side of the foundation if there is any loading. Lastly, the final bearing capacity of the foundation is determined by applying forced displacement. The analysis was conducted in terms of strength ratio, thickness ratio, and weak layer depth.

When a load or foundation is applied to soil, the stress it causes on the soil elements is not immediately known. However, a software solution can be used to determine the stresses resulting from the application of load or foundation by applying boundary conditions. For higher accuracy, 20-node elements were used in the analysis.

To capture the high stress gradient and the change in the direction of the principal stress, a very fine fan of elements at the edges of the footing was necessary. An illustration of the finite element mesh used in the analysis is shown in Figure 8.

The main parameters of soil behavior models are the mechanical characteristics of soil and rock, and these parameters (such as the modulus of elasticity E and internal friction angle ϕ of similar materials) find meaning

only in connection with the soil behavior models of similar materials because they must be kept unchanged during the calculations and Also, they should be independent of the problem, so they should be constant in mathematical equations. Model parameters for sand and clay are shown in Table 3.

Table 3. Model parameters for sand and clay

Soil	Parameter's	Poisson's ratio(ν)	Young's modulus (E)	Shear strength parameters		Dry unit weight γ (kn/m ³)
				Φ (deg)	C(kpa)	
Sand		0.30	40000	38	0	15.7
Clay		0.30	8000	28	0.35	12.2

In the present study, numerical modeling of a circular foundation with dimensions equal to the dimensions of the physical model was carried out. After finalizing the geometry of the model in Abaqus numerical software, the sections related to different layers are created and the relevant data of these sections are assigned to it. The Mohr-Coulomb constitutive model has been adopted and was used to define the characteristics of the same soil mass as mentioned earlier. for the software validation process, One of the models created by Ziccarelli and Rosone [21] who investigated the behavior of surface foundations in the presence of a weak layer using Plaxis 2D software, was investigated. In this manuscript, part of the study models of Ziccarelli and Rosone [21] where the friction angle of the weak layer is 10 degrees, the friction angle of the sand is 30 degrees, and the depth of the weak layer is modeled from 0.5 to 4B. The modeling results in this research and comparison with Ziccarelli and Rawson's research can be seen in Figure 7. In this figure, the horizontal axis is the ratio of the depth of the weak layer to the width of the foundation and the vertical axis is the ratio of the bearing capacity of the foundation in the presence of the weak layer (with variable depth and thickness) to the bearing capacity of the foundation on the uniform sand. As can be seen, as the depth of the weak layer increases, its effect on the bearing capacity decreases. In such a way that from a depth equal to 2.5B, the weak layer practically does not affect the bearing capacity. In addition, the results obtained from the modeling are completely similar to the findings obtained from the study of Ziccarelli and Rosone [21], which shows the correctness of the modeling process.

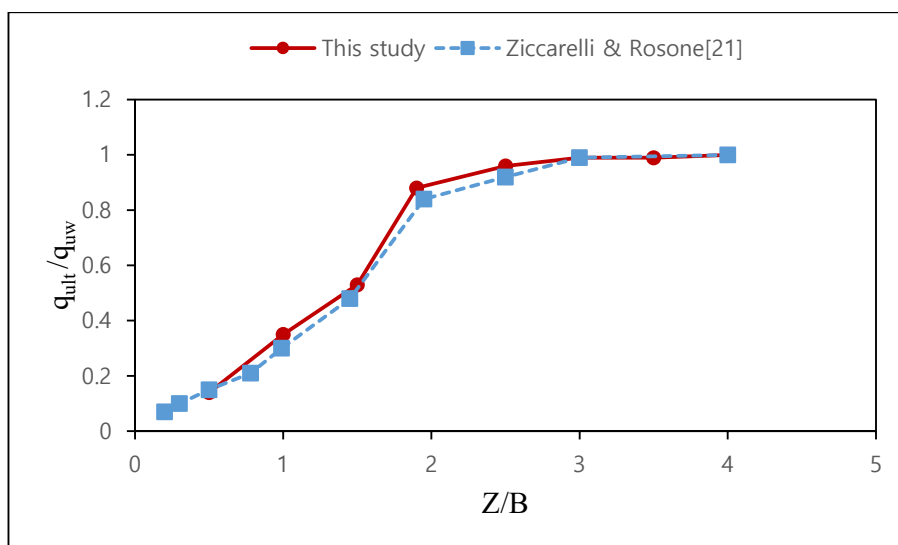


Figure 7. Normalised bearing capacity q_u/q_{uw} against normalised depth of the weak layer Z/B for this study compare with Ziccarelli and Rosone[21]

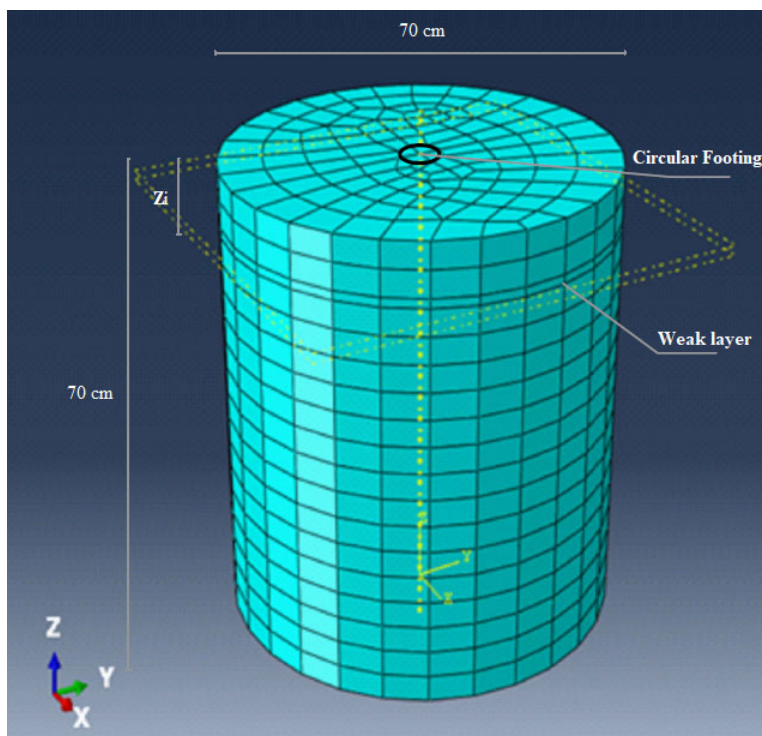


Fig 8. Illustration of the finite element mesh used for the circular foundations analysis.

5. Results and discussion

This study utilized a physical model to investigate the behavior of a circular foundation resting on a uniform sand bed, as well as on a sand bed with a weak layer at varying depths, thicknesses, and overburdens. The experimental program involved conducting twenty tests, with the variable parameters and values shown in Table 4, following the schematic diagram shown in Figure 2.

The experimental tests program for the circular foundation of the physical model is summarized in Table 4, and this information can be useful for further academic research in the field.

Test program conducted on a physical model of sand within a weak layer. The table includes 20 test cases, each identified by a test number and accompanied by three test data parameters: T , Z_i , and q' .

T , thickness of thin layer

Z_i , refers to the depth of the weak layer, measured in centimeters (cm).

q' , refers to the applied pressure on the footing, expressed as a fraction of the ultimate bearing capacity (q_{ult}) of the sand with a weak interlayer.

The purpose of the experimental test program was to investigate the behavior of the sand within the weak layer under various loading conditions, as reflected in the different combinations of T , Z_i , and q' for each test case. The results of these tests would likely be used to inform the development of a numerical model to further analyze the bearing capacity factors of the physical model.

Table 4. Experimental tests program on physical model of sand within weak layer

Test No	Test data
1	T=0, Z _i =0, q'=0
2	T=0, Z _i =0, q'=q _{ult}
3	T=0, Z _i =0, q'=2q _{ult}
4	T=0, Z _i =0, q'=3q _{ult}
5	T=7mm, Z _i =4cm, q'=0
6	T=7mm, Z _i =8cm, q'=0
7	T=14mm, Z _i =4cm, q'=0
8	T=14mm, Z _i =8cm, q'=0
9	T=7mm, Z _i =4cm, q'=q _{ult}
10	T=7mm, Z _i =4cm, q'=2q _{ult}
11	T=7mm, Z _i =4cm, q'=3q _{ult}
12	T=7mm, Z _i =8cm, q'=q _{ult}
13	T=7mm, Z _i =8cm, q'=2q _{ult}
14	T=7mm, Z _i =8cm, q'=3q _{ult}
15	T=14mm, Z _i =4cm, q'=q _{ult}
16	T=14mm, Z _i =4cm, q'=2q _{ult}
17	T=14mm, Z _i =4cm, q'=3q _{ult}
18	T=14mm, Z _i =8cm, q'=q _{ult}
19	T=14mm, Z _i =8cm, q'=2q _{ult}
20	T=14mm, Z _i =8cm, q'=3q _{ult}

The variable parameters and their values used in the model tests are presented below (table 5). The constant parameters were $D_r = 40\%$ and $D_f = 0$ for both test types. The tests were performed in two types: uniform sand and uniform sand with a weak layer.

Variable Parameters Values Test Type:

Z_i (depth of weak layer) 0, 4 cm, 8 cm Uniform sand with weak layer

T (thickness of weak layer) 7 mm, 14 mm Uniform sand with weak layer

q (applied load) 0, q, 2q, 3q Uniform sand and uniform sand with weak layer (for q values)

Table 5. Model test program

Type of test	Constant parameters	Variable parameters
Uniform sand	$D_r = 40\%, D_f = 0$	$z_i = 0$ $T = 0$ $q = q, 2q, 3q$
Uniform sand with weak layer	$D_r = 40\%, D_f = 0$	$z_i = 4, 8 \text{ cm}$ $T = 7, 14 \text{ mm}$ $q = q, 2q, 3q$

The pressure-settlement curve of a circular foundation resting on uniform sand soil is presented in Fig. 9, which shows that the ultimate bearing capacity of the foundation is 417.2 kPa. Different analytical methods, including Meyerhof [22], Vesic [23], and Hansen [24], were used to calculate the ultimate bearing capacity values corresponding to the stress level of the model, and the results are given in Table 6. It is observed that the bearing capacity obtained from the test is approximately 2.5 times greater than the Hansen [24] and Vesic [23] equations and smaller than the Meyerhof equation.

$$q_u = 0.3\gamma BN_y \text{ (Terzaghi [25])} \tag{1}$$

$$N_q = \tan^2 \left(45 + \frac{\phi}{2} \right) e^{\pi \tan \phi} \text{ (Meyerhof [22])} \tag{2}$$

$$N_y = (N_q - 1) \tan 1.4\phi \text{ (Meyerhof [22])} \tag{3}$$

$$N_y = 2(N_q + 1) \tan \phi \text{ (Vesic [23])} \tag{4}$$

$$N_y = 1.5(N_q - 1) \tan \phi \text{ (Hansen [24])} \tag{5}$$

Figures 11 show the bearing pressure-settlement curves of circular foundations resting on the sand bed with a weak layer at different thicknesses and depths. Fig 8 presents the results of the behavior of circular foundations with weak layers for different experimental modes. The results indicate that the absence of a weak layer in the soil mass increases the bearing capacity of the foundation. An increase in the value of surcharge load in Tests No. 2, 3, and 4 also increases the bearing capacity.

Table 6. Comparison of ultimate bearing capacity of circular footing Test No.1 with analytical relationships of various investigators

Test	Hansen	Meyerhof	Vesic
417.26	138.9	555	186.9

5.1 Reference state

Initially, the behavior of the reference state, where the circular footing is free from overburden and a weak lens, is examined. This case serves as the reference state for the analyses, and the change in bearing capacity with overburden or a weak interlayer is measured against this state. The reference state is designated as Test No. 1 in Table 3. The stress-strain curves in the numerical and experimental model for test No. 1 for the circular footing are depicted in Figure 9. The ultimate bearing capacity for this case is 417.26 kPa. Thus, in other tests detailed in Table 3, the value of q_{ult} is set to this amount. The bearing capacity for the assumed footing is provided in Table 6 using classical bearing capacity equations and the soil resistance parameters of sandy soil. It is observed that the bearing capacity obtained from the test is approximately 2.5 times greater than the Hansen [24] and Vesic [23] equations and smaller than the Meyerhof equation.

Although initially, the slope of the numerical curve is steeper and shows higher stiffness relative to the laboratory model, the ultimate bearing capacity calculated from the numerical model is 346.96 kPa, which is approximately 17% lower than the laboratory model. Hence, it can be concluded that the bearing capacity derived from the numerical and laboratory models is comparable, indicating the validity of the results. This case shows the correctness of the process followed in the numerical models.

Additionally, Figure 10 compares the results obtained by Marto et al. [26] with the results derived from this study. They examined the bearing capacity of circular footings on sandy beds in different soil densities and footing diameters statically. The soil they studied was classified as SP by the USCS, and the friction angle of the soil in one of the densities they examined was found to be 42.3 degrees, which is about 5 degrees smaller than the soil friction angle in this study. The first test by these researchers examines the behavior of a circular footing in a static state, which is similar to Test No. 1 in this research. The dimensionless bearing capacity chart (bearing capacity divided by the product of the specific weight and footing diameter) versus dimensionless settlement (settlement ratio to footing diameter) is observed in both tests. Generally, although the friction angle in these two studies differs by about 5 degrees, the dimensionless bearing capacity in this study is approximately 4.7 times greater than that of Marto et al.'s research. [26].

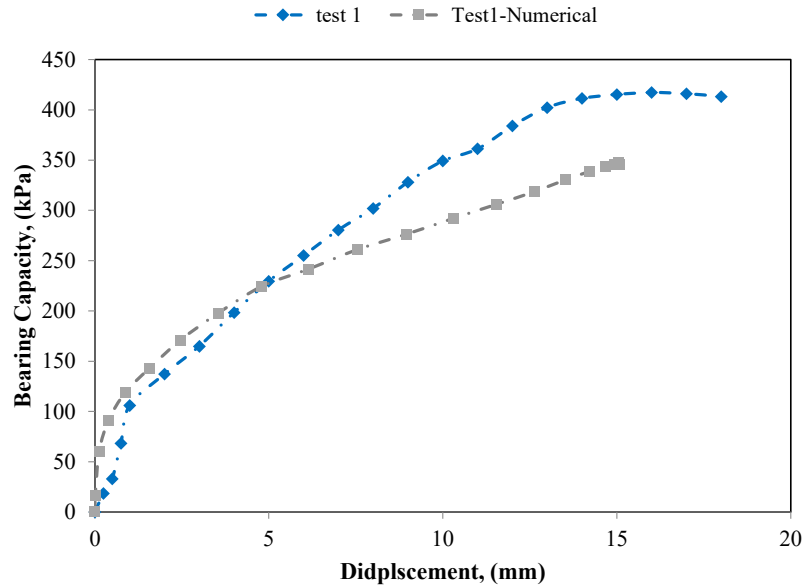


Fig 9. The stress-strain curves in the numerical and experimental model for test No. 1 for the circular footing

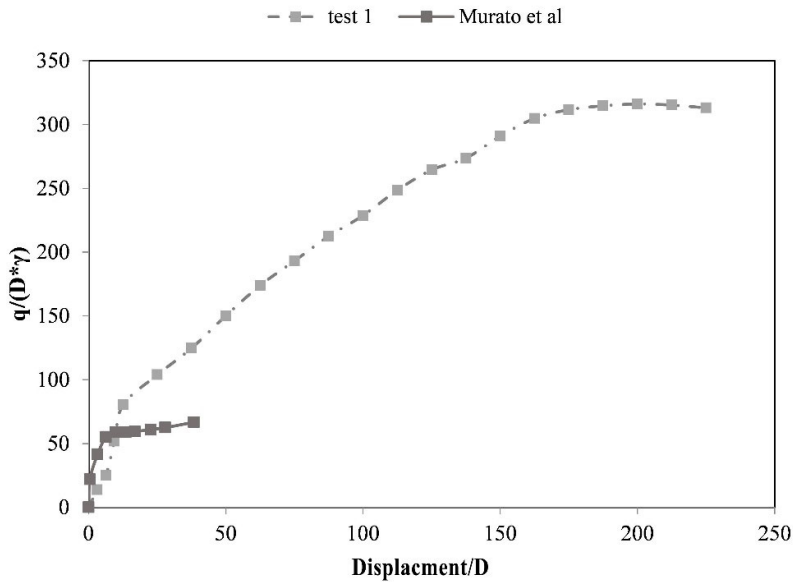


Fig 10. Comparison of Test No. 1 results with results from Murato et al. [26]

Figure 11, illustrates the displacement vector and shear strain created during failure in this experiment. As expected, in this model, the displacement vector and failure mechanism are symmetric relative to the central axis of the circular footing. Given the loading conditions and the uniformity of the footing, such behavior is anticipated.

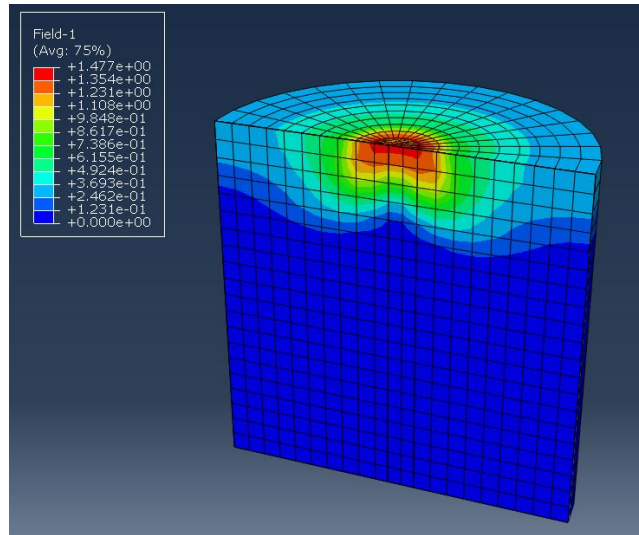


Fig 11. Displacement obtained from numerical model for Test No. 1 - circular footing

5.2 The impact of asymmetric loading without a weak lens

To examine the impact of asymmetric loading on the behavior of a circular footing situated on a homogeneous bed without a weak lens, the results from Tests No. 1 to 4 in Table 3 have been utilized. In these tests, asymmetric overburden was applied unilaterally as a percentage of the bearing capacity of the footing obtained from Physical Model No 1. The bearing capacity-settlement curves for these tests are shown in Figure 12.

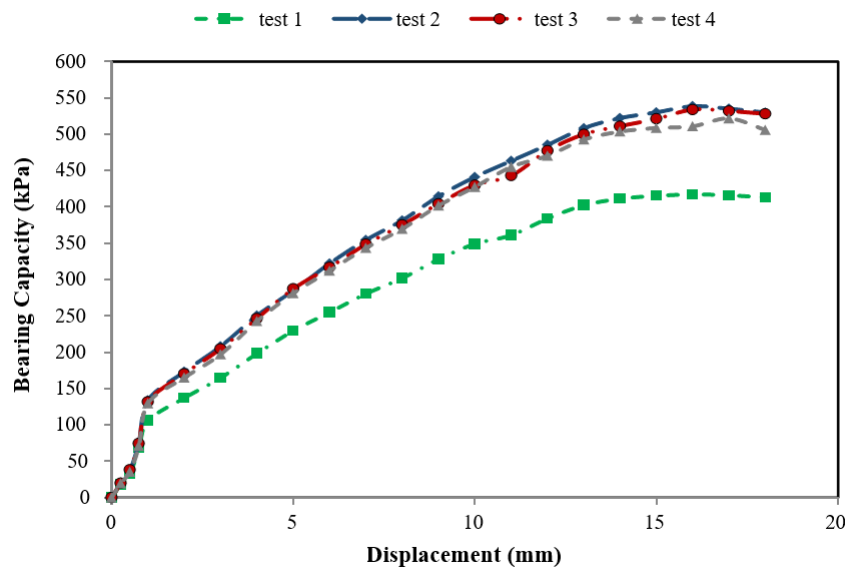


Fig 12. Bearing capacity-settlement curve for Tests No. 1 to 4 - strip footing

Additionally, the changes in ultimate bearing capacity in each test with the ratio of asymmetric overburden to the ultimate bearing capacity of Test No. 1 to 4 are shown in Figure 13. The ultimate bearing capacity is considered as the maximum sustainable stress. It is observed that with the application of asymmetric overburden equal to 1/3 of the ultimate load, the bearing capacity of the footing significantly increases from 417.26 kPa to 538.68 kPa, indicating an approximate 29% increase in ultimate bearing capacity. With the increase of the overburden to 1/2

and equal to the ultimate load, the ultimate bearing capacity respectively reaches 534.01 kPa and 521.99 kPa. This shows an approximate 28% and 25.1% increase in bearing capacity compared to the case without overburden.

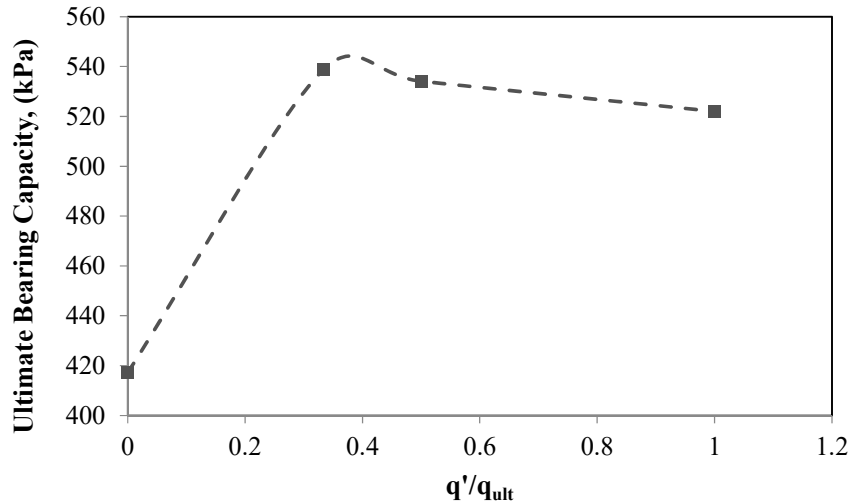


Fig 13. Variation of ultimate bearing capacity with asymmetric overburden ratio to ultimate bearing capacity, Tests No. 1 to 4

It is observed that the application of unilateral overburden generally leads to an increase in the bearing capacity of the circular footing. The most significant positive impact occurs when the overburden is 33% of the ultimate bearing capacity in the reference state. Further increasing the overburden slightly reduces the positive effect. The results of the numerical modeling for these tests are presented in Figure 14. It is noted that the initial slope of the curve in the numerical models is steeper than that in the physical models which indicates greater stiffness in the numerical models.

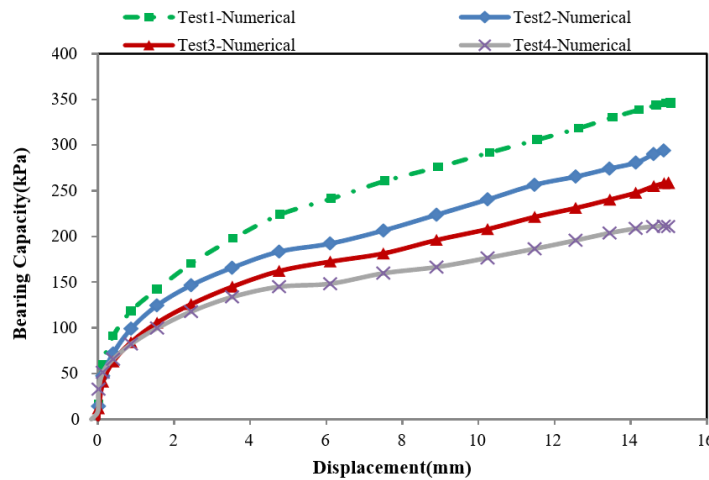


Fig 14. Bearing capacity-settlement curve obtained from the numerical model for Tests No. 1 to 4 - circular footing

To examine the effect of asymmetric overburden on the failure mechanism of circular footings, the results of the displacement vector in these tests are shown in Figure 15. It is observed that once asymmetric overburden is applied, the failure mechanism shifts from asymmetric state around the central axis and extends towards the side opposite to where the load is applied. The application of asymmetric overburden results in a deeper shear failure mechanism. This explains the increase in resistance with the increase in asymmetric overburden. The amount of asymmetric overburden is selected based on a coefficient of the bearing capacity of Test No. 1 (reference state) up to this level of asymmetric overburden has a positive effect on the bearing capacity and has not yet reached the critical asymmetric overburden. Regarding the mechanism of failure and its extension based on the results of

numerical modeling, it should be said that the asymmetric overburden causes the failure mechanism to be one-sided, which makes the mechanism out of the symmetrical state on the other hand, increases the expansion of the horizontal mechanism. The presence of the weak layer causes the failure mechanism to extend the weak layer and increases its depth. In general, the application of asymmetric overburden has a positive effect and shifts the failure mechanism from a symmetric state and makes it deeper.

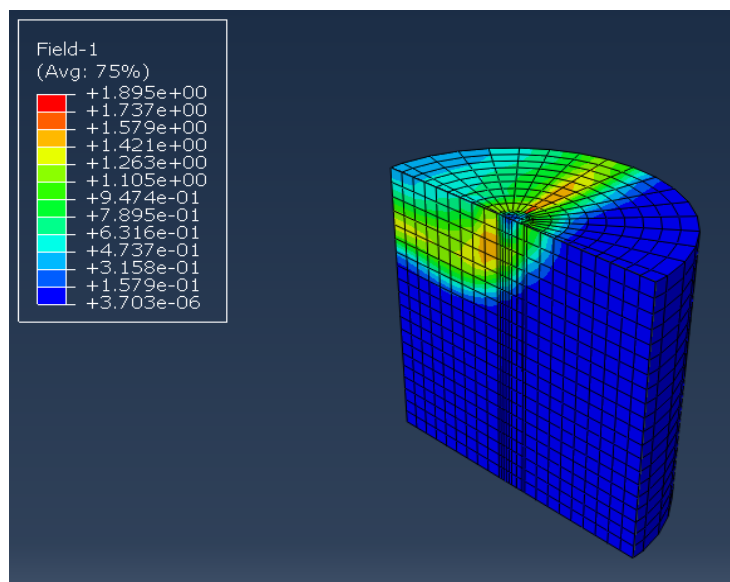


Fig 15. Displacement vector obtained from the numerical model for Test No. 2 - circular footing

5.3 The impact of weak lens presence without asymmetric loading

To examine the impact of a weak lens on the behavior of a circular footing without asymmetric loading, the results from Tests No. 1 and 5 to 8 have been utilized. In these experiments, a weak lens with thicknesses of 7 and 14 mm at depths of 4 and 8 cm from the ground surface was used to investigate the impact of the weak lens's depth and thickness. To prepare a uniform layer, sand rains from a certain height and at a constant rate of fall (according to the relative density of the sample, the drop height is determined) in layers of 4 to 5 cm inside the box. In the tests that include the weak layer, upon reaching the level of the weak layer, the layer of clay powder is made up to a certain thickness, and again the layers of sand are poured into the box until the final level is reached. The samples were made at a relative density of 40%. The bearing capacity-settlement curves from these experiments are shown in Figure 16, and Variation of ultimate bearing capacity with lens thickness or depth is depicted in Figure 17.

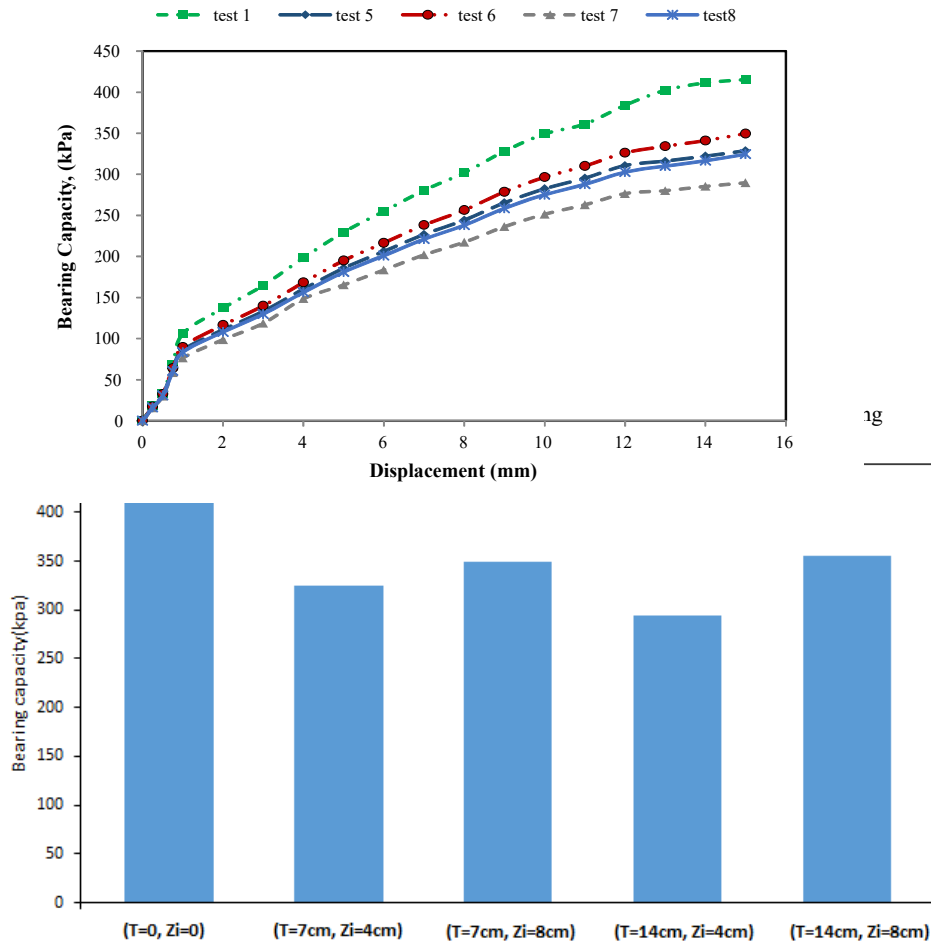


Fig 17. Variation of ultimate bearing capacity with lens thickness or depth, tests No. 1 and 5 to 8 - circular footing

According to the presence of a weak layer results in a substantial reduction in the ultimate bearing capacity of the footing. For a consistent depth, as the thickness of the weak layer increases, a further reduction in the ultimate bearing capacity is expected. For instance, in Tests 5 and 7, where the depth of the weak layer is 4 cm and its thicknesses are 7 and 14 mm, respectively, a decrease in bearing capacity of 21% and 28% compared to Test 1 is observed. These values increase to 14% and 19% in Tests 6 and 8, where the thicknesses of the lens are 4 and 8 mm, respectively, but the depth is 7 cm. On the other hand, increasing the depth of the weak layer reduces its negative effect. Additionally, a comparison of these experiments indicates that regardless of the depth of the weak layer, the bearing capacity of the circular footing decreases. However, as the weak layer gets deeper, its impact becomes less significant.

The results of the numerical modeling for these experiments are depicted in Figure 18. It is noted that the initial slope of the curve in the numerical models is greater than that in the physical models which indicates greater stiffness in the numerical models. The difference in numerical modeling values compared to physical modeling shows the dependence of the shear strength angle on the stress level. The extension of the failure mechanism in the numerical analysis was very close to the results of the physical model, and the influence of the weak layer and asymmetric overburden was similar in the physical and numerical models, which is significantly effective in the extension and depth of the mechanism. Additionally, the ultimate bearing capacities resulting from the numerical models, physical models and conventional bearing capacity equations are provided in Table

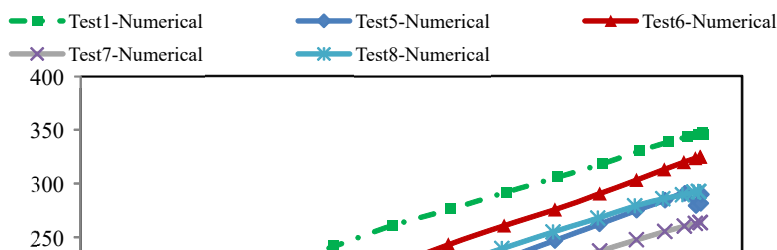


Fig 18. Bearing capacity-settlement curve obtained from numerical model for Tests No. 1 and 5 to 8 - circular footing

Table 7. Bearing capacity obtained from Tests 1 and 5 to 8 for circular footings with values derived from numerical modeling and classical bearing capacity equations, in kPa

Test NO.	Physical Model	Numerical Model	Hansen	Meyerhof	Vesic
1	417.26	346.0	138.9	555	186.9
5	328.80	289.89	447.1	161	233.4
6	356.09	324.82	447.1	161	233.4
7	298.87	271.77	363.2	139.5	192.8
8	334.36	308.89	363.2	139.5	192.8

The bearing capacity for Test No. 5 in the numerical model is 289.89 kPa, which indicates a difference of 11.8% compared to the physical model. For Tests No. 6, 7 and 8, the bearing capacities obtained from the numerical model are 324.82 kPa, 271.77 kPa and 308.89 kPa, respectively, showing differences of 8.8%, 9.1% and 7.6% compared to the physical model results. Hence, the results from the physical and numerical models are consistent with each other. However, there is a significant discrepancy between the results from these two methods and the classical bearing capacity equations. It is important to note that the classical bearing capacity results are obtained by averaging the parameters of the bed and the lens in the active zone underneath the footing. This discrepancy can be explained by the fact that in conventional methods, averaging the parameters does not significantly affect the reduction of resistance parameters because the thickness of the weak layer is negligible. Consequently, there is no considerable reduction in bearing capacity observed in these methods. In practice, however, the weak layer leads to a change in the failure mechanism.

5.4 The impact of weak lens presence with asymmetric loading

To investigate this case, the results from Tests No. 1 and 9 to 20 have been utilized. The ultimate bearing capacity curves from these tests are depicted in Figure 19. In all cases, the obtained bearing capacity is lower than in the initial state, which is due to the presence of the weak lens. Based on the results, the following points can be made:

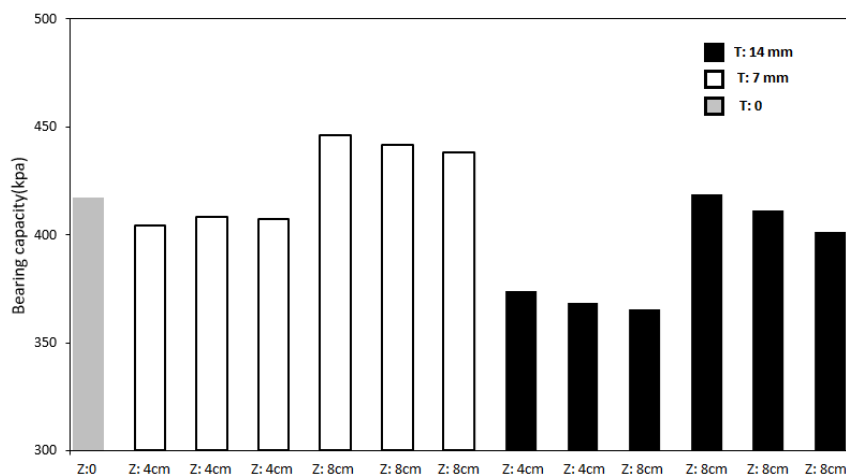


Fig 19. Variation of ultimate bearing capacity with lens thickness or depth and asymmetric overburden, Tests No. 1 and 9 to 20 - circular footing

- Under identical conditions of weak lens thickness and depth, increasing the asymmetric overburden increases bearing capacity in bearing capacity. For example, comparing Test 5 with Tests 9 to 11 illustrates this clearly, as the 21% reduction in bearing capacity in the absence of overburden decreases to a 3% reduction with the minimum applied overburden stress. There is no significant difference between the various levels of overburden.
- Under the same loading and lens depth conditions, an increase in the thickness of the weak clay lens results in a greater reduction in bearing capacity. For instance, comparing Tests 9 with 15 and Tests 11 with 17 exhibits a 10% greater reduction in bearing capacity with an increased lens thickness under identical conditions.
- Under the same loading and lens thickness conditions, as the depth of the weak clay lens increases, its impact on bearing capacity decreases. For example, comparing Tests 9 with 12 and Tests 10 with 13 shows a decrease in the effect of the weak lens on bearing capacity as its depth increases.
- Comparing the bearing capacity in the presence of a weak clay lens with and without asymmetric overburden indicates that the existence of asymmetric overburden on one side of the footing significantly reduces the negative effect of the lens. In scenarios where a lens is present without overburden, the bearing capacity of the circular footing decreases by 14% to 28%, depending on the lens thickness and depth. However, with asymmetric overburden the reduction in capacity is less than 10% even at the minimum applied values, indicating the significant impact of asymmetric overburden.
- It can be noted that asymmetric loading has a more substantial effect on the bearing capacity of the circular footing when no clay lens is present. Without the lens, asymmetric overburden leads to a 25% to 29% increase in bearing capacity. However, with the lens present at various thicknesses and depths, the increase in bearing capacity due to asymmetric overburden ranges from 15% to 20% compared to the state without overburden.

The results of the numerical modeling for these tests are presented in Figure 20. It is noted that the initial slope of the curve in the numerical models is steeper than in the physical models, indicating greater stiffness in the physical models.

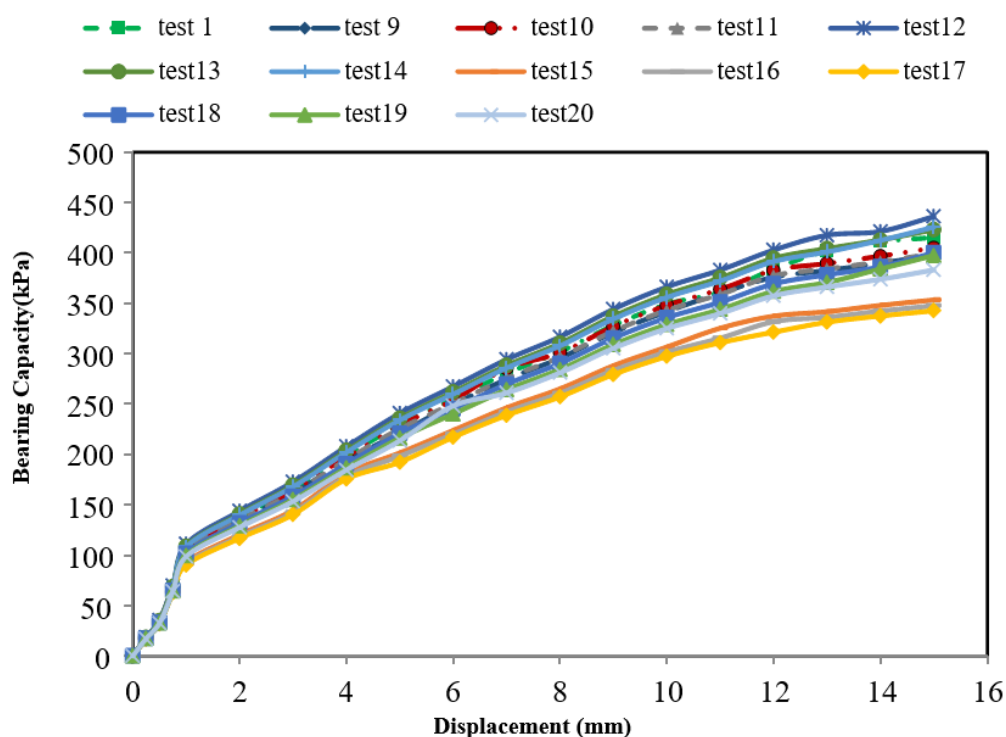


Fig. 20 Bearing capacity-settlement curve obtained from numerical modeling for Tests No. 1 and 9 to 20 - circular footing

Previous studies have mainly focused on investigating the impact of weak layers on strip foundations on soil layers. However, studying different types of foundation and footing geometries is crucial to better understand the behavior of soil layers under various loading conditions. In this regard, exploring the effect of weak layers on circular foundations is particularly important, and this study has provided valuable insights in this area. Furthermore, it is essential to investigate the influence of weak layer thickness and depth on the bearing capacity of the foundation, as well as the positive and negative effects of their location. The present study has also examined the impact of overburden magnitude on the ultimate bearing capacity of the foundation. In light of the above, we can improve our understanding of soil behavior and make more accurate predictions about the behavior of foundations in different scenarios.

6. Conclusions

In conclusion, the results of this study demonstrate that the presence of a weak clay layer has a significant effect on the bearing capacity of circular footings. The thickness and depth of the weak layer have a considerable impact on the ultimate bearing capacity of the foundation, and can increase the bearing capacity. The experimental results indicate that the highest value of bearing capacity has a 30% improvement compared to the test with no weak layer, and has a 27% decrease in the ultimate bearing capacity of the circular footing at the maximum decrease.

The experimental evidence also shows that adding overburden pressure to the physical models with a weak layer can prevent some of the negative effects of its existence. The overburden pressure in one side of footing increase the bearing capacity about 12 to 18 % according to the pressure.

The investigation of the impact of the thickness and depth of the weak layer location and its positive or negative effects on the bearing capacity of the foundation is also of particular importance. Moreover, the study provides valuable information on the effects of overburden magnitude on the ultimate bearing capacity of the foundation. The results suggest that the overburden has a significant effect on the bearing capacity and can be used to prevent some of the negative effects of weak layer existence. In this study, both numerical and experimental analyses were conducted to evaluate the bearing capacity of circular footings on layered soil with weak layers. Both results are in good agreement.

The experimental results, as presented in Table 7, showed that the bearing capacity of the circular footing decreased as the thickness of the weak layer increased. The numerical results, as presented in Table 7, also showed a similar trend, where the bearing capacity decreased with the increasing thickness of the weak layer. Furthermore,

the load-settlement curves obtained from the experimental and numerical analyses showed a similar trend for the footings on layered soil with and without weak layers. In both cases, the addition of a weak layer resulted in a decrease in the bearing capacity of the footing, the tests were performed at a relative density of 40%.

Overall, the results from both the experimental and numerical analyses are consistent with each other, indicating that the presence of a weak layer has a significant impact on the bearing capacity of circular footings on layered soil. The results from this study can provide valuable information for the design and construction of foundations in areas with layered soil and weak layers.

References

- [1] Ahmad, MA. and Khalafalla, AH. (2019). *Numerical investigation of the bearing capacity of shallow foundations on layered soils with weak layers*. Alexandria Engineering Journal, 58(4), 1271-1284
- [2] Amin, MT. and Adhikary, S. (2019). *Effect of overburden pressure on bearing capacity of shallow footings on layered soils*. Geomechanics and Engineering, 18(1), 1-13
- [3] Arora, KR. Sharma, AK. and Kumar, D. (2017). *Bearing capacity of circular footing on layered soil with a weak layer*. Journal of Rock Mechanics and Geotechnical Engineering, 9(2),377-382.
- [4] Behera, RN. Patra, CR. Das, BM. and Sivakugan, N. (2018). *Ultimate bearing capacity of shallow strip foundation under eccentrically inclined load—a critical assessment*. International Journal of Geotechnical Engineering, 15(7), 897–905
- [5] Abd Elaziz, M., Elghazouli, A., and Elsanadedy, H. (2016). *Bearing capacity of shallow foundations on soft and weak soils in Egypt*. Alexandria Engineering Journal, 55(3), 1973-1983.
- [6] Al-Sammaraie, AM. and Al-Rawas, AA. (2019). *Effect of weak layer parameters on the bearing capacity of strip footings on layered soils*. Geomechanics and Engineering, 17(5), 425-439.
- [7] Huang, C-C. (2019). *Effects of restraining conditions on the bearing capacity of footings near slopes*. Soils and Foundations, 59(1), 1-12
- [8]. Khamehchiyan, M. Charkhabi, A. and Tajik, M. (2007). *Effects of Crude Oil Contamination on Geotechnical Properties of Clayey and Sandy Soils*. Engineering Geology, (89), 220–229.
- [9] Ullah, SN., Stainer, S., HU, Y. and White, D. (2017). *Foundation punch-through in clay with sand: analytical modelling*. Géotechnique 2017; 67(8), p. 672-6.91
- [10] Mahboubi Niazmandi, M. (2023) *Estimation of the undrained bearing capacity of strip foundations on two-layer clay soils adjacent to the geogrid-stabilized slope under the effect of combined loading*. Journal of Structural and Construction Engineering, 11(3). doi: 10.22065/jsce.2023.402512.3146
- [11] Mahboubi Niazmandi, M., Mirasi, S., Hashemi joker, M. and Momeni, M. (2023). *The effect of combined loading on the bearing capacity of strip footings located on two-layered clayey soils adjacent to geogrid-reinforced slopes*. Amirkabir Journal of Civil Engineering, 55(9),1825-1844. doi: 10.22060/ceej.2023.21741.7812
- [12] Singh Yadav, J., Saini, A., Hussain, S. and Sharma, V. (2024). *Estimation of ultimate bearing capacity of circular footing resting on recycled construction and demolition waste overlaying on loose sand*. Journal of Building Pathology and Rehabilitation. <https://doi.org/10.1007/s41024-023-00378-z>
- [13] Bhardwaj, A. and Sharma, RK. (2023). *Experimental and Numerical Investigations on the Bearing Capacity of Footings on the Layered Soil*. International Journal of Geosynthetics and Ground Engineering, 9, 35. <https://doi.org/10.1007/s40891-023-00461-y>
- [14] Buragadda, V., Thyagaraj, T., Dhiman, R., Reddy Orekanti, E. and Kumar Maddileti, T. (2024). *Influence of Geosynthetic Reinforcement Geometrical Parameters on Load-Bearing Capacity of Sand: An Experimental Study*. Transportation Infrastructure Geotechnology, <https://doi.org/10.1007/s40515-024-00416-4>
- [15] Eshkevari, SS., Abbo, AJ. and Kouretzis, G. (2019). *Bearing capacity of strip footings on layered sands*. Computers and Geotechnics, Volume 114
- [16] Hanna, A., Abou Farah, C. and Abdel-Rahman M. (2020). *Shallow foundations resting on strong sand overlaying weak sand*. Journal of engineering and applied science, 67 (6),1399-1414
- [17] Haghsheno, H., Jamishidi Chenari, R. and Javankhoshdel, S. (2020). *Seismic Bearing Capacity of Shallow Strip Footings on Sand Deposits with Weak Inter-layer*. Geotech Geol Eng, (38), 6741–6754
- [18] Peng, M-X. and Peng, H-X. (2019). *The ultimate bearing capacity of shallow strip footings using slip-line method*. Soils and Foundations, 59(3), 601-616.
- [19] Bildik, S. and Laman, H. (2015). *Experimental investigation of the effects of pipe location on the bearing capacity*.

Geomechanics and Engineering, 8(2), 221-235

- [20] Bakhshandeh, M. and Mahboubi Niazmandi, M. (2023). *Seismic Response of Base-Isolated Irregular Steel Structures Equipped with Lead-Rubber Bearing Isolators Considering the Effects of Soil-Structure Interaction*. International Review of Civil Engineering, 14 (6), 464-478. <https://doi.org/10.15866/irece.v14i6.22871>
- [21] Zicarelli, M. and Rosone, M. (2021). *Influence of a Thin Horizontal Weak Layer on the Mechanical Behaviour of Shallow Foundations Resting on Sand*. Geosciences, 11(9), 392
- [22] Meyerhof, GG. (1957). *The Ultimate Bearing Capacity of Foundations on Slopes*. 4th International Conference on Soil Mechanics and Foundation Engineering, (3), 384-386
- [23] Vesic, AS. (1973) *Analysis of ultimate loads of shallow foundations*. Journal of the soil mechanics and foundations division, (99), 45 -73
- [24] Hansen, JB. (1963) *A General Formula for Bearing Capacity*. Danish Geotechnical Institute, Copenhagen
- [25] Terzaghi, K. (1963). *Theoretical Soil Mechanics*. Wiley
- [26] Marto, A., Oghabi, M. and Mohd Yunus, NZ. (2015). *Bearing capacity of Circular footing on Sand Deposit*. Applied Mechanics and Materials, (773),1518-1523
- [27] Mahboubi Niazmandi, M. (2023) *Estimation of the undrained bearing capacity of strip foundations on two-layer clay soils adjacent to the geogrid-stabilized slope under the effect of combined loading*. Journal of Structural and Construction Engineering,11(3). doi: 10.22065/jsce.2023.402512.3146